

Fig. S1. Comparison validation of Transpiration Fraction (TF) from GLEAM and SiTHv2 datasets. (a) Natural Forest and (c) Planted Forest TF temporal correlation. The legend shows the Pearson correlation coefficient (R) for the growing season TF time series (1990-2020) from GLEAM and SiTHv2 at each pixel. Black dots indicate pixels that passed the significance test ($p < 0.05$). (b) Natural Forest and (d) Planted Forest TF spatial comparison. (b) and (d) are density scatter plots comparing the multi-year mean TF values from SiTHv2 (y-axis) and GLEAM (x-axis). The black dashed line is the 1:1 line, and the blue solid line is the linear regression line. The correlation coefficient (R), Root Mean Square Error (RMSE), Bias, and total pixel count (N) are provided.

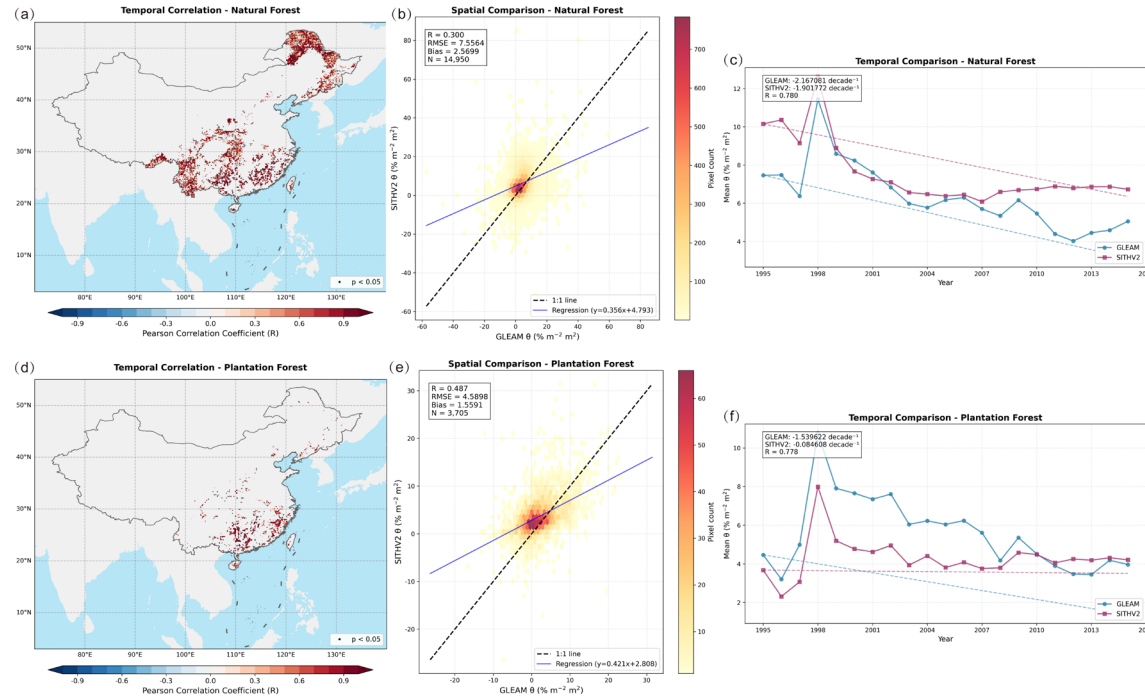


Fig. S2. Comparison validation of LAI-TF sensitivity (θ) from GLEAM and SiTHv2 datasets. (a) Natural Forest and (d) Planted Forest θ temporal correlation. The legend shows the Pearson correlation coefficient (R) for the growing season θ time series at each pixel. Black dots indicate pixels that passed the significance test ($p < 0.05$). (b) Natural Forest and (e) Planted Forest θ spatial comparison. (b) and (e) are density scatter plots comparing the multi-year mean θ values from SiTHv2 (y-axis) and GLEAM (x-axis). The black dashed line is the 1:1 line, and the blue solid line is the linear regression line. The correlation coefficient (R), Root Mean Square Error (RMSE), Bias, and total pixel count (N) are provided. (c) Natural Forest and (f) Planted Forest θ temporal comparison. (c) and (f) show the interannual variation of the mean θ for both forest types from 1995-2015. The pink (GLEAM) and blue (SiTHv2) solid lines are the interannual values, and the dashed lines are their respective linear trend lines, annotated with the decadal trend slope (decade^{-1}) and R^2 .

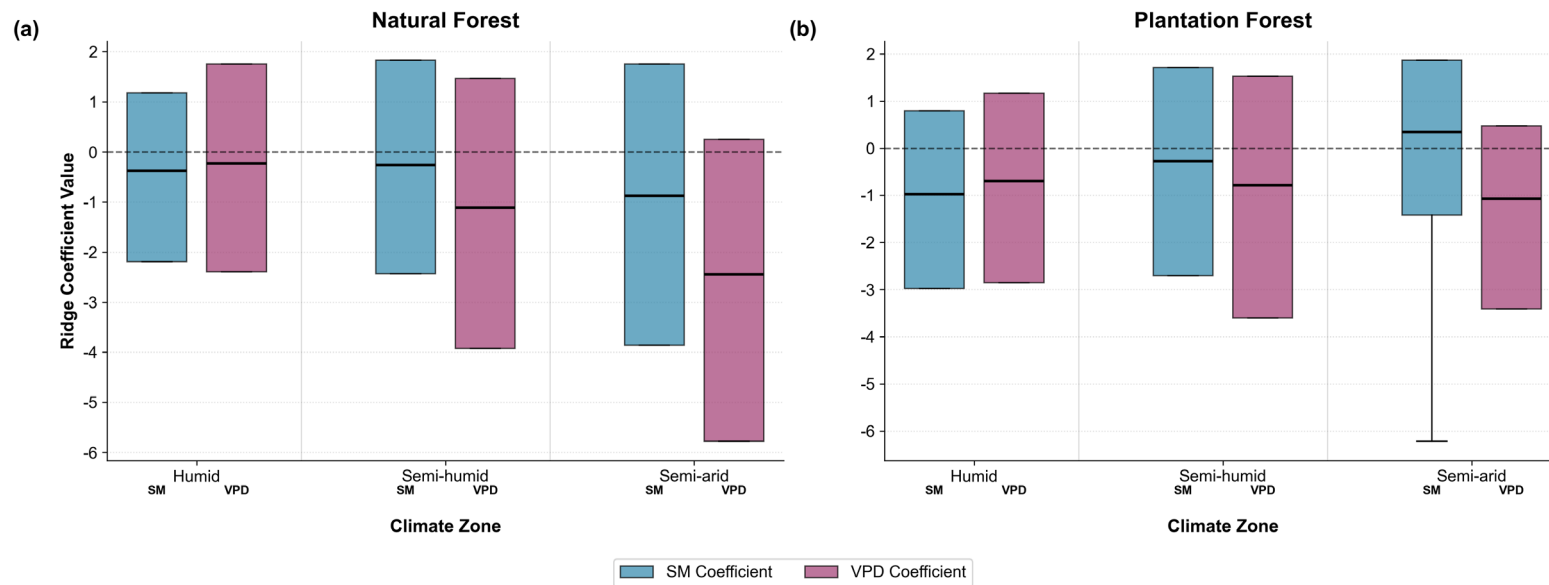


Fig. S3. Distribution of ridge regression coefficients (β) in different climatic zones for Natural and Planted Forests. (a) Natural Forest and (b) Planted Forest boxplots of standardized ridge regression coefficient values in the three climatic zones (Humid, Semi-humid, Semi-arid). The boxes show the 25th percentile, median, and 75th percentile of the β coefficients, with whiskers extending to the minimum and maximum data values. Blue boxes represent the SM coefficient (β_{SM}), and magenta boxes represent the VPD coefficient (β_{VPD}).

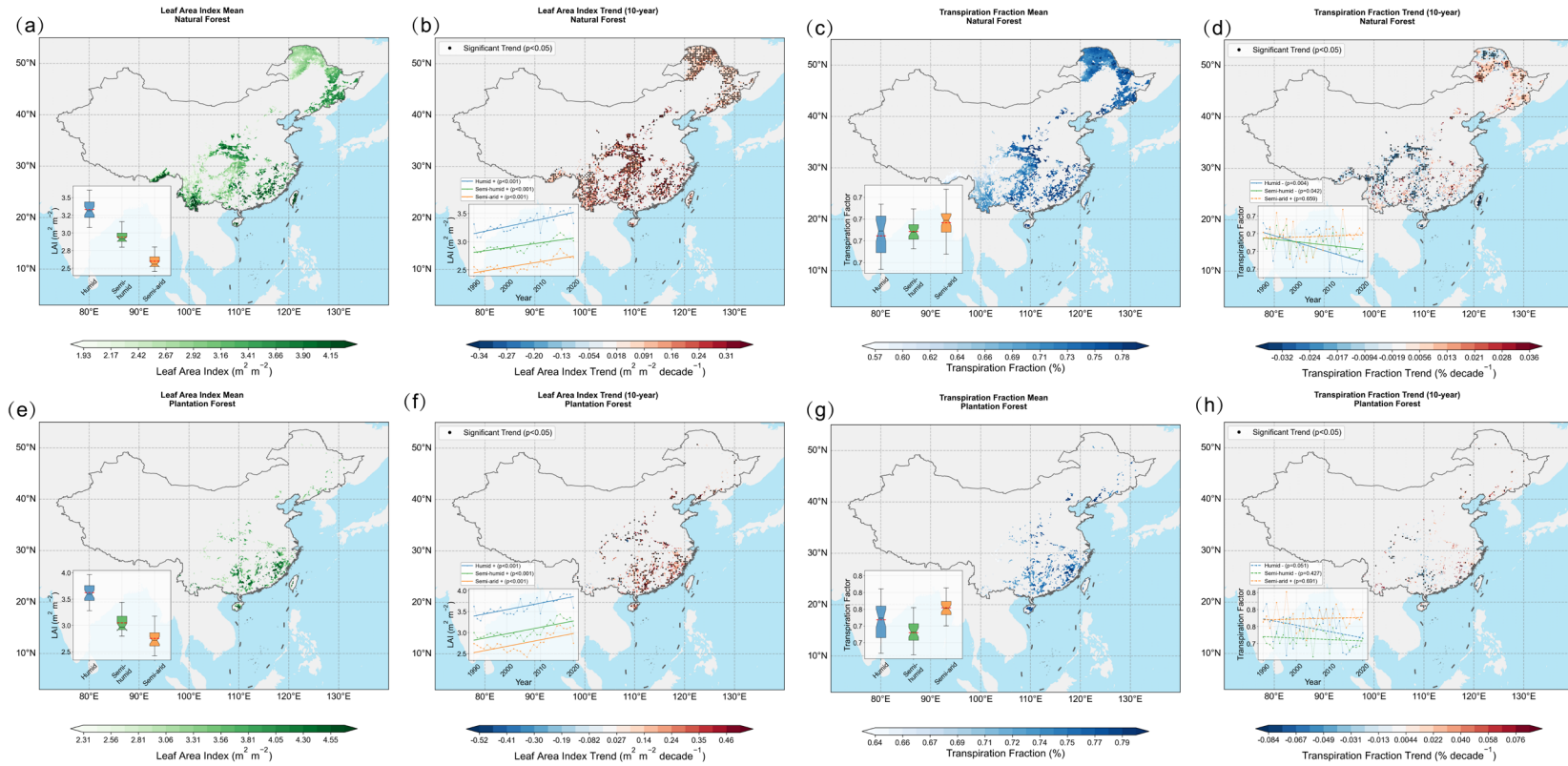


Fig. S4. Spatial patterns and temporal trends of Leaf Area Index (LAI) and Transpiration Fraction (TF) for China's Natural and Planted Forests. Top row (a-d) is for Natural Forest, bottom row (e-h) is for Planted Forest. (a, c, e, g) show the multi-year mean spatial distribution of LAI and TF, respectively. Inset plots are boxplots of LAI or TF statistics for different climatic zones (Humid, Semi-humid, Semi-arid). (b, d, f, h) show the change trends for the corresponding metrics, with only significantly tested areas ($p < 0.05$) marked. Inset plots show the interannual changes of LAI or TF for different climatic zones.

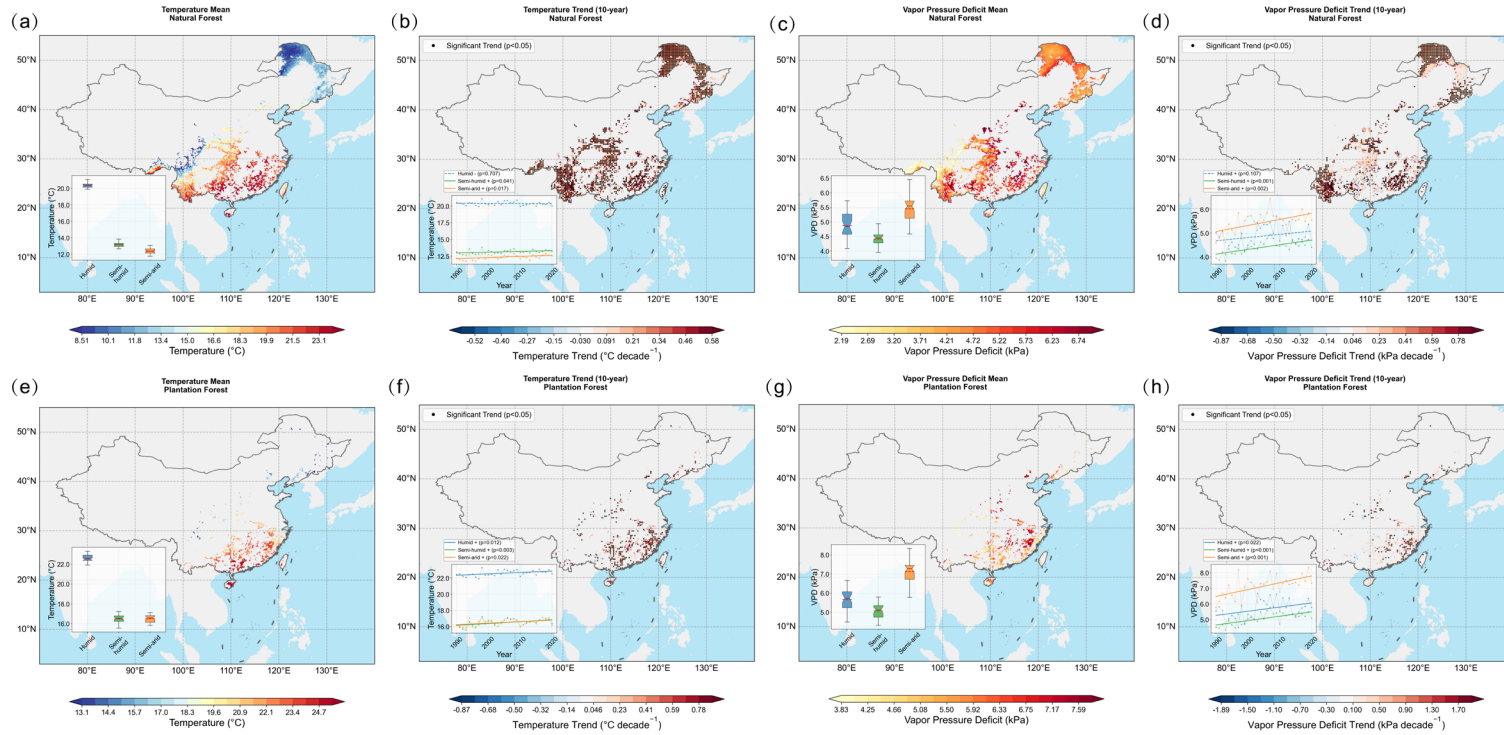


Fig. S5. Spatial patterns and temporal trends of Air Temperature (Ta) and Vapor Pressure Deficit (VPD) for China's Natural and Planted Forests. Top row (a-d) is for Natural Forest, bottom row (e-h) is for Planted Forest. (a, c, e, g) show the multi-year mean spatial distribution of temperature and VPD, respectively. Inset plots are boxplots of temperature or VPD statistics for different climatic zones (Humid, Semi-humid, Semi-arid). (b, d, f, h) show the change trends for the corresponding metrics, with only significantly tested areas ($p < 0.05$) marked. Inset plots show the interannual changes of temperature or VPD for different climatic zones.

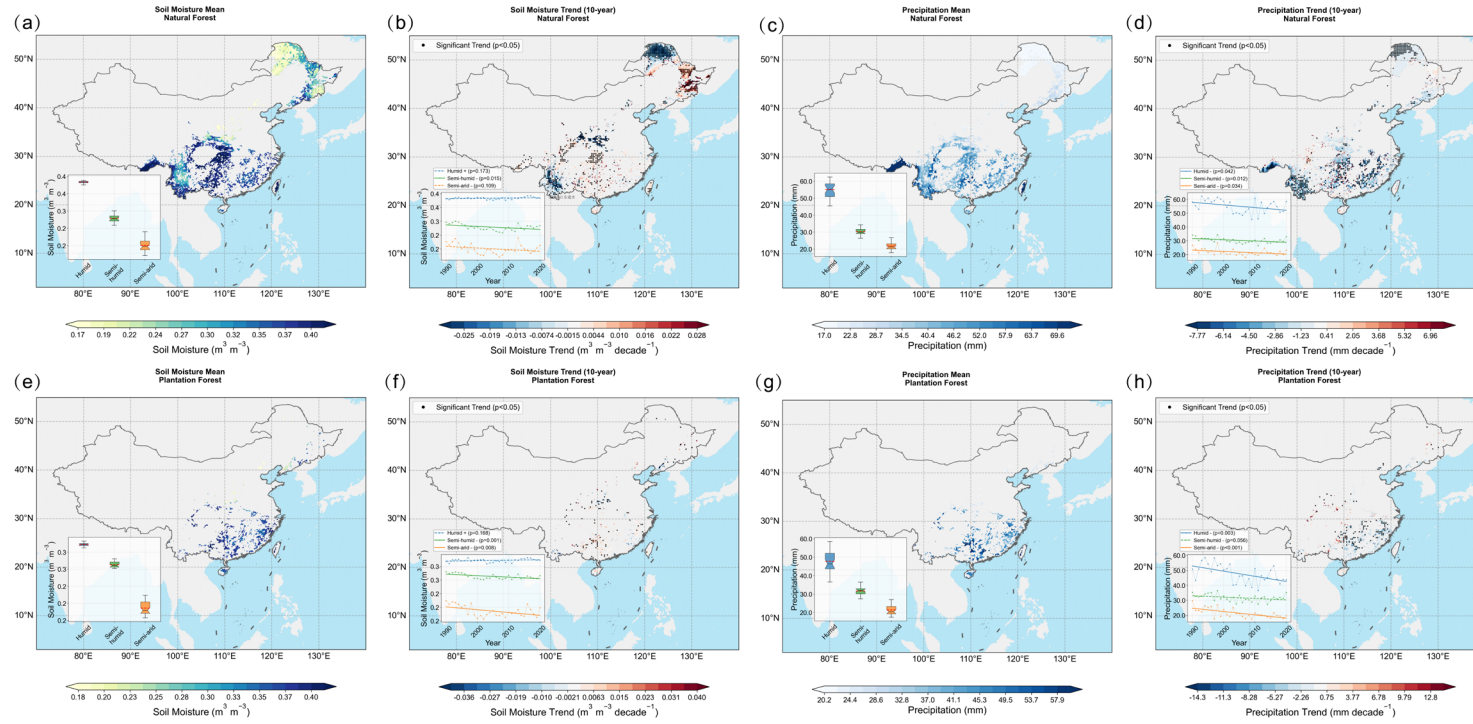


Fig. S6. Spatial patterns and temporal trends of Soil Moisture and Precipitation for China's Natural and Planted Forests. Top row (a-d) is for Natural Forest, bottom row (e-h) is for Planted Forest. (a, c, e, g) show the multi-year mean spatial distribution of soil moisture and precipitation, respectively. Inset plots are boxplots of soil moisture or precipitation statistics for different climatic zones (Humid, Semi-humid, Semi-arid). (b, d, f, h) show the change trends for the corresponding metrics, with only significantly tested areas ($p < 0.05$) marked. Inset plots show the interannual changes of soil moisture or precipitation for different climatic zones.

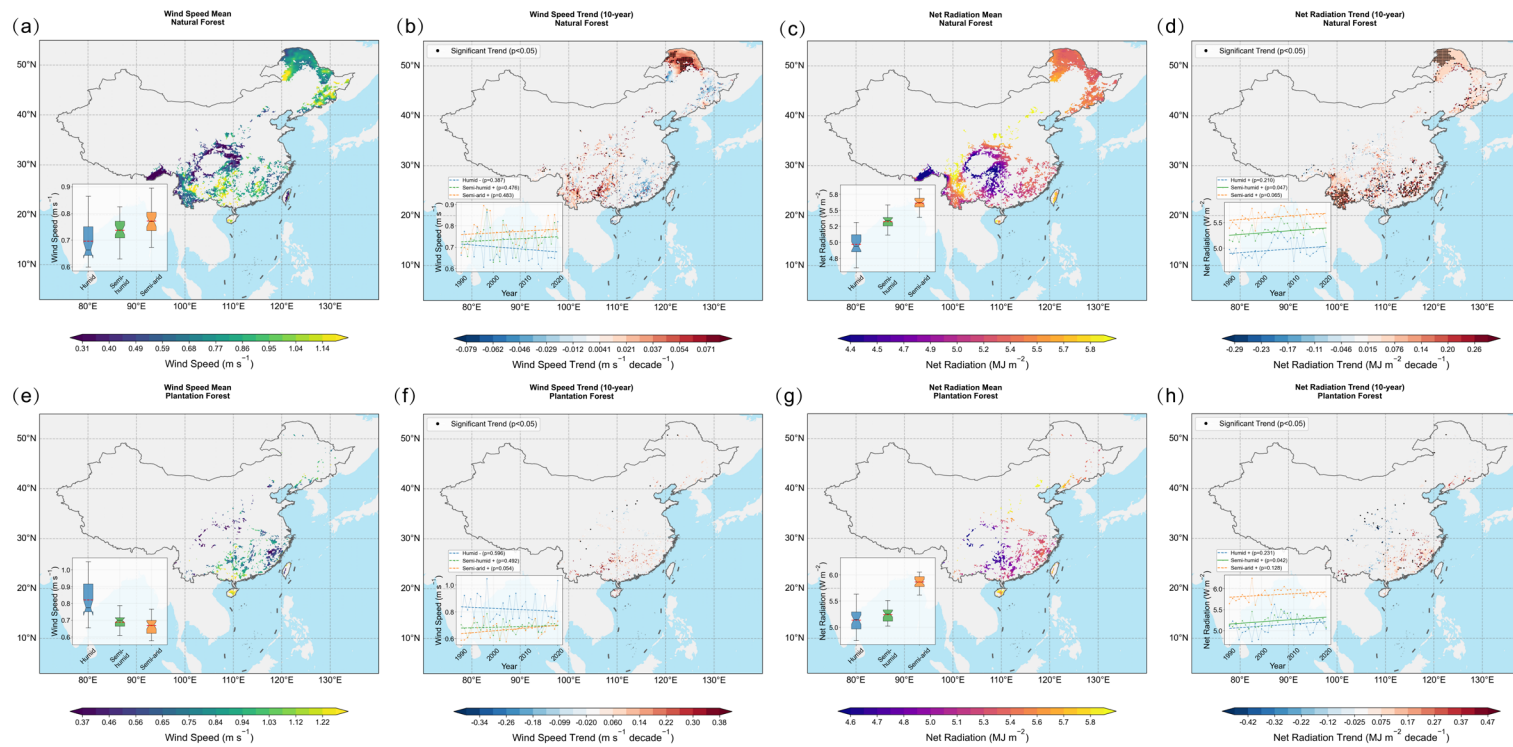


Fig. S7. Spatial patterns and temporal trends of Wind Speed and Net Radiation for China's Natural and Planted Forests. Top row (a-d) is for Natural Forest, bottom row (e-h) is for Planted Forest. (a, c, e, g) show the multi-year mean spatial distribution of wind speed and net radiation, respectively. Inset plots are boxplots of wind speed or net radiation statistics for different climatic zones (Humid, Semi-humid, Semi-arid). (b, d, f, h) show the change trends for the corresponding metrics, with only significantly tested areas ($p < 0.05$) marked. Inset plots show the interannual changes of wind speed or net radiation for different climatic zones.

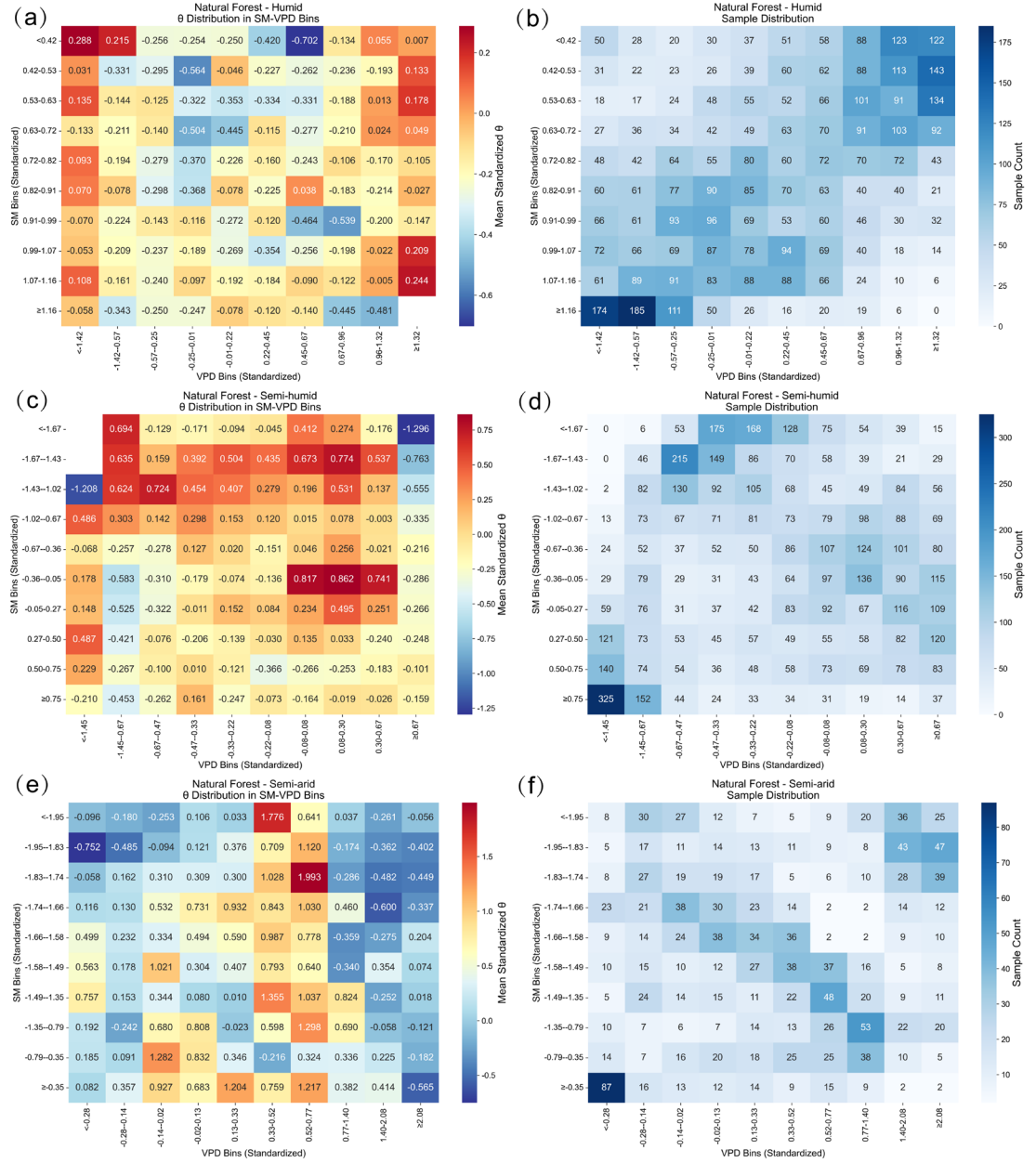


Fig. S8. Pooled spatial results of forest LAI—TF sensitivity (θ) under Soil Moisture (SM) and Vapor Pressure Deficit (VPD) bins for Natural Forests in different climatic zones. (a, b): Humid zone, (c, d): Semi-humid zone, (e, f): Semi-arid zone. The left column of heatmaps shows the mean θ value within different SM and VPD combination intervals, with color indicating the magnitude of θ . The right column of heatmaps shows the data sample size within each combination interval.

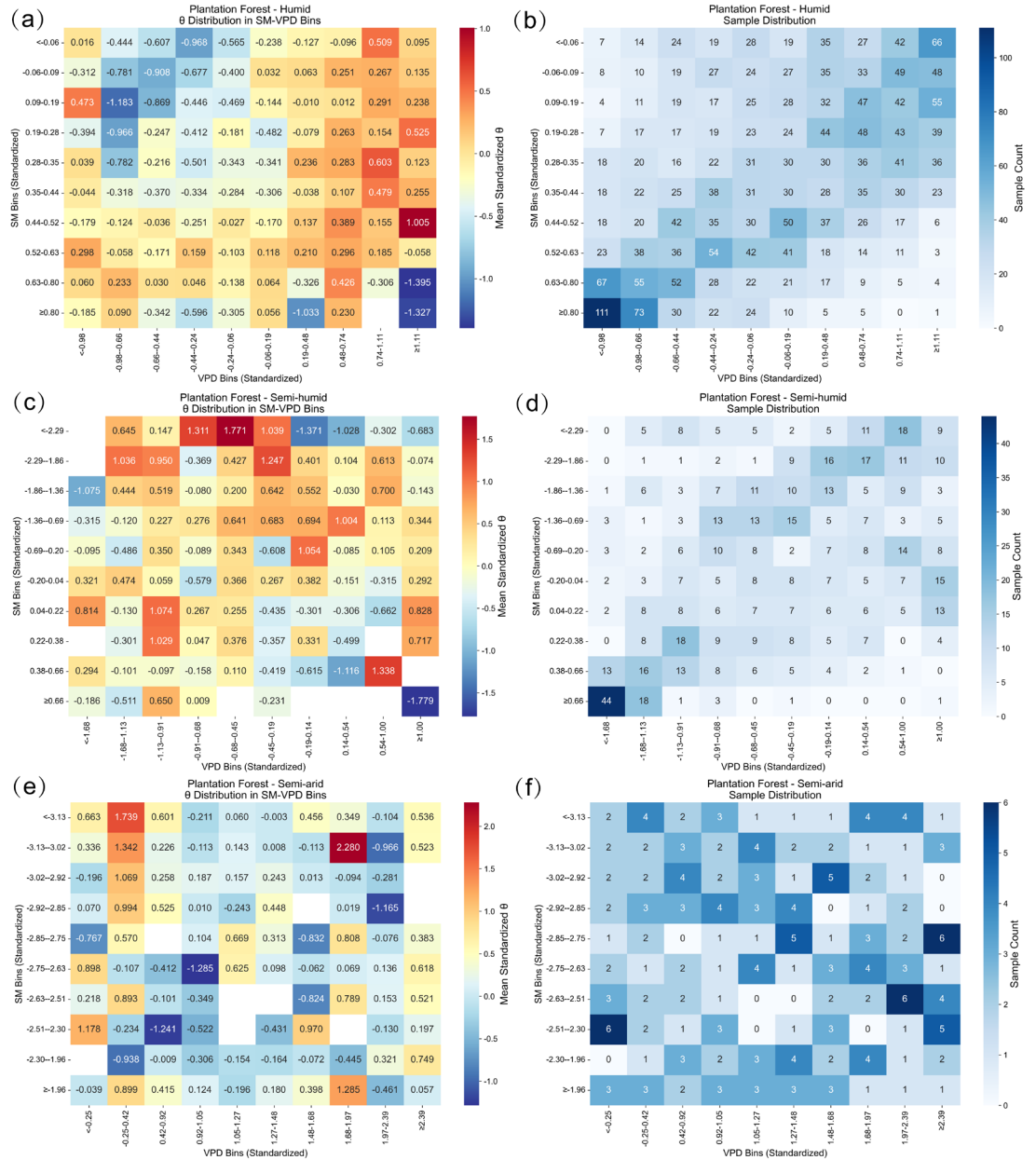


Fig. S9. Pooled spatial results of forest LAI—TF sensitivity (θ) under Soil Moisture (SM) and Vapor Pressure Deficit (VPD) bins for Planted Forests in different climatic zones. (a, b): Humid zone, (c, d): Semi-humid zone, (e, f): Semi-arid zone. The left column of heatmaps shows the mean θ value within different SM and VPD combination intervals, with color indicating the magnitude of θ . The right column of heatmaps shows the data sample size within each combination interval.